

A NOVEL TPC CONVERTER FOR HYBRID RENEWABLE ENERGY SYSTEM

Mr.M.Sivaraman, M.E,Assistant Professor,Department of Electrical and Electronics

PSR Engineering college, Sivakasi.

Mr.K.Kanagaraj PG Scholar, PSR Engineering College ,Sivakasi.

ABSTRACT:

A new partly isolated three-port converter is introduced in this study for hybrid energy applications. Two boost circuits form the main input port and a bidirectional battery port of the converter. Therefore, both of them are of a current-fed type, making the converter more suitable for renewable energy applications. In addition, the boost circuits are benefited from a mutual active clamp circuit. The circuit in cooperation with the leakage inductance of transformers provides soft switching, while employing a few number of semiconductors. Furthermore, on the secondary side, two voltage-doubler rectifiers are merged. As a result, the converter employs less number of components, but participating in all power conversion modes. Since most of the renewable energy sources have a relatively low voltage level, the converter retains high voltage gain. These features have resulted in an efficient and inexpensive converter.

I. INTRODUCTION

The advent of Three-Port Converters (TPCs) has pushed the hybrid energy systems toward higher power density, in the recent decade. A conventional hybrid system utilizes, at least, two converters (one for output voltage adjustment and the other for power regulation); however, a TPC has merged them into one. Generally, a TPC has a main input, a main output and a bidirectional port. Adequate power management ability is a very basic incentive for designing a TPC. A typical TPC must be able to control the power flow among the ports to respond to the demanded power properly, while regulating the output voltage.

Typically, TPCs can be divided into three categories as, isolated, non-isolated, and partly-

isolated [3]. In an isolated TPC (ITPC), all of the three ports are isolated from each other, using one or two transformers, and in most cases, it is composed of some full/half-bridge converters and rectifiers [4-9]. Therefore, power can easily be managed among the ports. In such condition, when the power is exchanged between two ports, the third one is idle and non-operational components are unavoidable. An ITPC uses full-scale high-frequency transformers to increase the voltage gain [5-6] which increases the converter's weight, size and magnetic losses.

Partly-Isolated TPCs (PITPCs) use a partial scale transformer to isolate one port (often the main output port) [25-34]. In addition, the leakage inductance of the transformer provides the possibility to achieve soft-switching [27-34]. Even though a transformer has been utilized, the voltage gain of PITPCs generally is low [22-31]. None of the mentioned references has current-fed ports and the number of semiconductors is high.

From the topological viewpoint, a PITPC can be flexible enough to merit the advantages of the both isolated (such as soft switching and high voltage gain) and non-isolated (such as a satisfactory component sharing and few semiconductors) TPCs [3]. Thus, a PITPC is proposed to address most of the features mentioned above. The proposed converter in this study presents a high voltage gain, and shares almost all the components in all operation modes. The number of semiconductors is reduced significantly in comparison with the other PITPCs, while all of them operate under soft-switching condition. Two boost circuits are employed to form two current-fed ports.

II. RELATED WORK:

S. S. Dobakhshari, et. al., (2017) proposed a quasi-resonant dc-dc converter with high voltage

gain and low current stresses on switches. This converter preserved inherent advantages of current-fed structures, for instance, zero magnetizing dc offset, low input ripple, and low transformer turn ratio. Moreover, by employing the active-clamp circuit, the voltage spikes across the main switch, due to the existence of leakage inductance of the isolating transformer, is absorbed, and switches work in zero voltage switching. Since quasi-resonant switching strategy is employed, turn-off current (TOC) and losses of switches are considerably reduced.

Y.-M. Chen, et. al., (2002) proposed a multi-input DC/DC power converter based on the flux additivity. Instead of combining input DC sources in the electric form, the proposed converter combines input DC sources in magnetic form by adding up the produced magnetic flux together in the magnetic core of the coupled transformer. With the phase-shifted pulsewidth-modulation (PWM) control, the proposed converter can draw power from two different DC sources and deliver it to the load individually and simultaneously.

Wang, et. al., (2012) proposes a new asymmetrical duty cycle control method for a three-port bidirectional DC-DC converter with two current-fed ports interfacing with low voltage battery and ultracapacitor in a fuel cell vehicle. Along with the phase shift control managing the power flow between the ports, asymmetric duty cycle is applied to each port to maintain a constant DC bus voltage at low voltage side, which as a result will achieve wide zero-voltage-switching (ZVS) range for each port under varied ultracapacitor and battery voltages. The ZVS range analysis of different duty cycle control methods as well as the circulation power loss between the ports have been analyzed.

III. SYSTEM IMPLEMENTATION

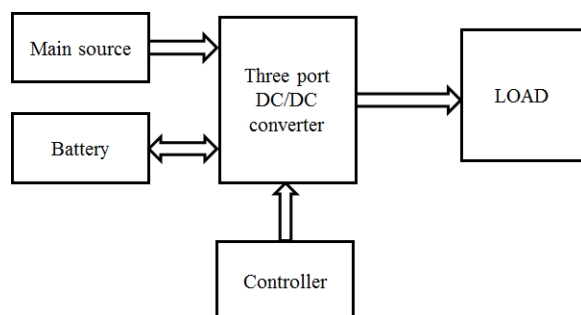


Fig.1 Proposed Block diagram

The proposed block diagram is shown in figure 1. The main source and battery source is connected to load through three port DC/DC converter. Battery is connected to converter bidirectional for charging and discharging purpose.

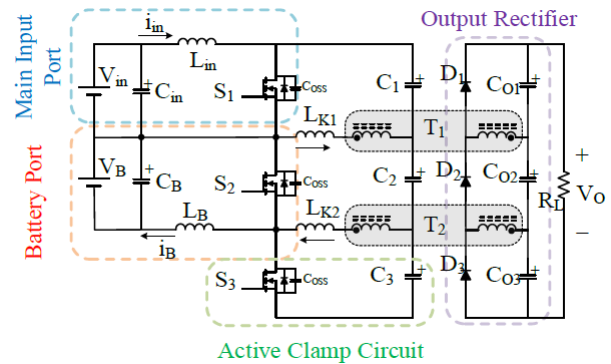


Fig.2 The proposed PITPC topology

Fig.2 shows the proposed PITPC, which is composed of two boost circuits (V_{in} , S_1 , L_{in} , C_1 and V_B , S_2 , L_B , C_2). S_3 and C_3 operate as a mutual active clamp circuit for the boost circuits. Two transformers isolate the output port and increase the voltage gain. L_{k1} and L_{k2} are the corresponding leakage inductances of the transformers. At the output, D_1 , D_2 , D_3 and C_{O1} , C_{O2} , C_{O3} , form a rectifier, which is resulted from two merged voltage-doublers. In addition, the load is modeled as R_L . The operation principles of the proposed PITPC in Double-input-single-output (DISO) mode, Single-input-single-output (SISO) mode, and Single-input-double-output (SIDO) mode, are explained in the following. In DISO mode, the main input and the battery port deliver the demanded power to the load. In SISO mode, the battery is idle and the input port transfers power to the load. In SIDO mode, the battery is charging and it acts as an output. The key waveforms of the converter in these modes are depicted in Fig. 3. As shown in Fig. 2, in DISO mode, gate-pulses of S_1 and S_3 (V_{GS1} and V_{GS3}) are complementary, and V_{GS2} leads V_{GS3} , by $d_2 d T_s$. When d_2 decreases to zero, V_{GS2} and V_{GS3} become synchronous and complementary with V_{GS1} . As a converter goes to SIDO mode. The pulsewidth of S_1 is defined as $d_1 T_s$. S_2 and S_3 have the same pulse width as $(1-d_1) T_s$. In this analysis, it is assumed that the voltage of all the capacitors and

current of input inductors are constant. Furthermore, switches and diodes are considered ideal.

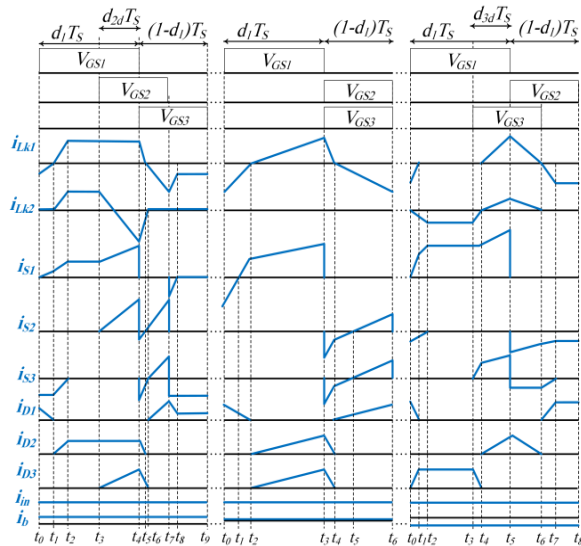


Fig. 3 key waveforms of the proposed PITPC in (a) DISO mode, (b) SISO mode, (c) SIDO mode.

1. OPERATIONAL PRINCIPLES OF THE PROPOSED PITPC

Fig.1 shows the proposed PITPC, which is composed of two boost circuits (V_{in} , S1, Lin, C1 and VB, S2, LB, C2). S3 and C3 operate as a mutual active clamp circuit for the boost circuits. Two transformers isolate the output port and increase the voltage gain. Lk1 and Lk2 are the corresponding leakage inductances of the transformers. At the output, D1, D2, D3 and CO1, CO2, CO3, form a rectifier, which is resulted from two merged voltage-doublers. In addition, the load is modelled as RL. The operation principles of the proposed PITPC in Double-input-single-output (DISO) mode, Single-input-single-output (SISO) mode, and Single-input-double-output (SIDO) mode, are explained in the following. In DISO mode, the main input and the battery port deliver the demanded power to the load. In SISO mode, the battery is idle and the input port transfers power to the load. In SIDO mode, the battery is charging and it acts as an output. The key waveforms of the converter in these modes are depicted in Fig. 2. As shown in Fig. 2, in DISO mode, gate-pulses of S1 and S3 (V_{GS1} and V_{GS3}) are complementary, and V_{GS2} leads V_{GS3} , by d_2dTs . When d_2 decreases to zero, V_{GS2} and V_{GS3} become synchronous and complementary with

V_{GS1} . As a result, the converter enters to SISO mode. In addition, When V_{GS3} leads V_{GS2} , by d_3dTs , the converter goes to SIDO mode. The pulse width of S1 is defined as d_1Ts . S2 and S3 have the same pulse width as $(1-d_1)Ts$. In this analysis, it is assumed that the voltage of all the capacitors and current of input inductors are constant. Furthermore, switches and diodes are considered ideal.

A. DISO Mode:

According to the waveforms in Fig. 3, converter's operation in this mode is divided into nine intervals.

Interval 1 [t_0 - t_1]: At t_0 , S1 turns ON and makes a cut-set containing Lk1, Lin and LB. Since the inductor current cannot change immediately, i_{S1} smoothly rises from zero. Therefore, the switch turns ON with Zero Current Switching (ZCS). In this interval, i_{Lk1} is negative, so D1 is conducting on the secondary side. When this current reaches zero, D1 turns OFF under ZCS and this interval ends. The battery port current (I_B) flows through the body diode of S3.

Interval 2 [t_1 - t_2]: At t_1 , i_{Lk2} and i_{Lk1} rise from zero with the same slope; consequently, D2 turns ON in the secondary side. When i_{Lk2} equals I_B , i_{S3} comes to zero and this interval ends.

Interval 3 [t_2 - t_3]: In this interval, i_{Lk1} and i_{Lk2} are equal to I_{in} and I_B , respectively. This interval lasts until the gate-pulse of S2 is applied.

Interval 4 [t_3 - t_4]: At t_3 , S2 turns ON. Since S3 is OFF and S2 is in a cut-set containing LB and Lk2, its current rises gradually from zero. Therefore, S2 turns ON under ZCS. In this interval, i_{Lk2} decreases but i_{Lk1} is still constant. This inequality turns D3 ON on the secondary side. Also, i_{S1} and i_{S2} increase.

Interval 5 [t_4 - t_5]: At t_4 , S1 goes OFF. Since S1 and S3 are in a cut-set containing some magnetic components, when S1 turns OFF, its current flows through the body diode of S2 and S3. This condition provides ZVS turn ON for S3 in this interval. At the end of this interval, i_{D2} descends to zero and D2 turns OFF under ZCS.

Interval 6 [t5-t6]: In this interval, switches have the same condition as in the previous interval. However, at t_5 , D2 turns OFF and D1 turns ON. At the end of this interval, i_{Lk2} reaches zero. Consequently, D3 turns OFF under ZCS in the secondary side.

Interval 7 [t6-t7]: At t_6 , the direction of i_{S3} changes and flows through the switch. In addition, i_{Lk2} remains zero, so D2 and D3 are kept OFF. At t_7 , gate-pulse of S2 is removed and this interval finishes.

Interval 8 [t7-t8]: At t_7 , S2 turns OFF; thus, i_{S3} suddenly changes, because i_{LB} has to flow through the body diode of S3. Moreover, $i_{Lk1}+i_{LB}-i_{Lin}$ flows through the body diode of S1, because these currents cannot change immediately.

Interval 9 [t8-t9]: In this interval, S1 and S2 are turned OFF while i_{LB} is still flowing through the body diode of S3 and $i_{LB}-i_{Lin}$ is passing through Lk1. At t_9 , gate-pulse of S3 is removed and this interval ends.

B. SISO Mode:

According to the waveforms in Fig. 3, the PITPC's operation in this mode is divided into six intervals.

Interval 1 [t0-t1]: At t_0 , S2 and S3 turn OFF and $i_{Lk1}-i_{in}$ flows through the body diode of S1, making it ready to be turned ON under ZVS. This interval finishes when this current comes to zero. Because of the negative current in Lk1, D1 is conducting on the secondary side.

Interval 2 [t1-t2]: At t_1 , i_{S1} changes direction and flows through the switch. At the end of this interval, when i_{Lk1} goes to zero, D1 turns OFF under ZCS.

Interval 3 [t2-t3]: At the beginning of this interval, the direction of i_{Lk1} changes. As a result, the current direction in the secondary side changes, and D2 and D3 turn ON.

Interval 4 [t3-t4]: At t_3 , S1 turns OFF and its current is diverted to the body diodes of S2 and S3, making them ready to turn-on under ZVS. At t_4 , i_{Lk1} reaches

zero, again. Therefore, D2 and D3 turn OFF under ZCS.

Interval 5 [t4-t5]: At t_4 , the direction of i_{Lk1} changes, which turns D1 ON. The rest of the converter's components operate the same as in the previous interval.

Interval 6 [t5-t6]: At t_5 , the direction of i_{S2} and i_{S3} change and they flow through the switches. This interval finishes when gate-pulses of S2 and S3 are removed.

C. SIDO Mode:

According to the waveforms in Fig. 3, the PITPC's operation is divided into eight intervals in the SIDO mode.

Interval 1 [t0-t1]: At t_0 , S1 turns ON. Since it is in a cut-set containing some magnetic components, it turns ON under ZCS. At the end of this interval, i_{Lk1} reaches zero as well as i_{D1} in the secondary side. Thus, D1 turns OFF under ZCS.

Interval 2 [t1-t2]: At t_1 , i_{Lk1} remains zero, and i_{S1} increases. At the end of this interval, i_{Lk2} reaches IB. As a result, i_{S2} goes to zero.

Interval 3 [t2-t3]: In this interval, i_{in} and i_B flow through S1 and Lk2, respectively. This interval ends when the gate-pulse of S3 is applied.

Interval 4 [t3-t4]: At t_3 , S3 turns ON. In this interval, since S2 is OFF and S3 is connected to a node with LB and Lk2, i_{S3} rises gently from zero. Therefore, S3 turns ON under ZCS. Meanwhile, i_{Lk2} declines to zero and turns D3 OFF under ZCS.

Interval 5 [t4-t5]: At t_4 , D2 and D3 turn ON and OFF, respectively, and i_{Lk1} and i_{Lk2} ascent from zero with the same slope. This interval finishes when gate-pulse of S1 is removed.

Interval 6 [t5-t6]: At t_5 , S1 turns OFF. Therefore, i_{S1} becomes zero and the current is transferred to the body diodes of S2 and S3. At this time, the direction of i_{S3} changes instantly. At the end of this interval,

leakage currents come to zero and D2 turns OFF under ZCS.

Interval 7 [t6-t7]: At t6, the direction of i_{Lk1} changes, consequently, D1 starts conduction. At the end of this interval i_{Lk1} becomes equal to I_{in} .

Interval 8 [t7-t8]: At t7, i_{S3} becomes zero and S3 turns OFF. Thus, I_{in} and I_B flow through L_{k1} and body diode of S2, respectively.

IV. HARDWARE PRESENTATION

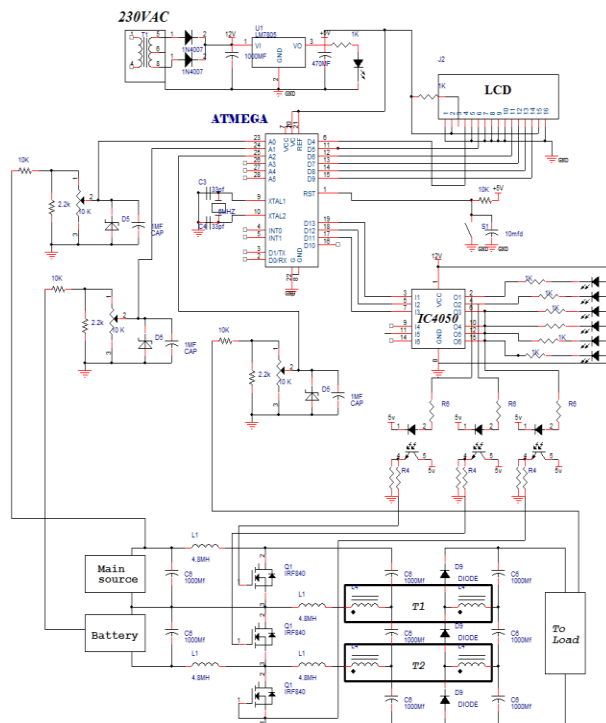


Fig. 4 Hardware circuit

The above figure.4 represents the hardware circuit for three port converter. The power supply gives supply to all components. It is used to convert AC voltage into DC voltage. Transformer used to convert 230V into 12V AC. 12V AC is given to diode. Diode range is 1N4007, which is used to convert AC voltage into DC voltage. LM 7805 regulator is used to maintain voltage as constant. Then signal will be given to next capacitor, which is used to filter unwanted AC component. Load will be LED and resistor. LED voltage is 1.75V. if voltage is above level beyond the limit, and then it will be dropped on resistor. The microcontroller is connected with LM7805 regulator out at port Vcc, Vref, RST. The driver requires a 12V supply. The main source

and battery source is connected to load through three port DC/DC converter. Battery is connected to converter bidirectional for charging and discharging purpose. In our proposed system we design a three port converter using embedded controller. We are using Atmega328 for performing control operation by using the MOSFET switches. For switching we are using MOSFETs. Which are connected to the microcontroller through Optocoupler. The Optocoupler are used for avoiding rapidly changing voltages on one side of the circuit from damaging components or distorting transmissions on the other side. It is connected to controller through buffer. Buffer IC4050 used for store the data. The proposed PITPC, which is composed of two boost circuits (V_{in} , S1, L_{in} , C1 and VB, S2, LB, C2). S3 and C3 operate as a mutual active clamp circuit for the boost circuits. Two transformers isolate the output port and increase the voltage gain. L_{k1} and L_{k2} are the corresponding leakage inductances of the transformers. At the output, D1, D2, D3 and CO1, CO2, CO3, form a rectifier, which is resulted from two merged voltage-doublers. In addition, the load is modeled as RL. In this project also monitor the voltages from main source and battery and also measured the load voltage by using voltage measuring unit.

1. PIC16F877A Controller

PIC 16F877 is one of the most advanced microcontroller from Microchip. This controller is widely used for experimental and modern applications because of its low price, wide range of applications, high quality, and ease of availability. It is ideal for applications such as machine control applications, measurement devices, study purpose, and so on.

Why PIC is used?

- High speed
- High performance RISC (Reduced Instruction Set Computer) CPU
- Instruction Set simplicity
- Integration of operation features
- Programmable timer options
- Interrupt control
- EPROM/OTP/ROM options
- Inbuilt modules
- Low power consumption
- Wide operation voltage range: 2.5 to 6 volt
- Programmable code protection mode

- Power saving sleep mode

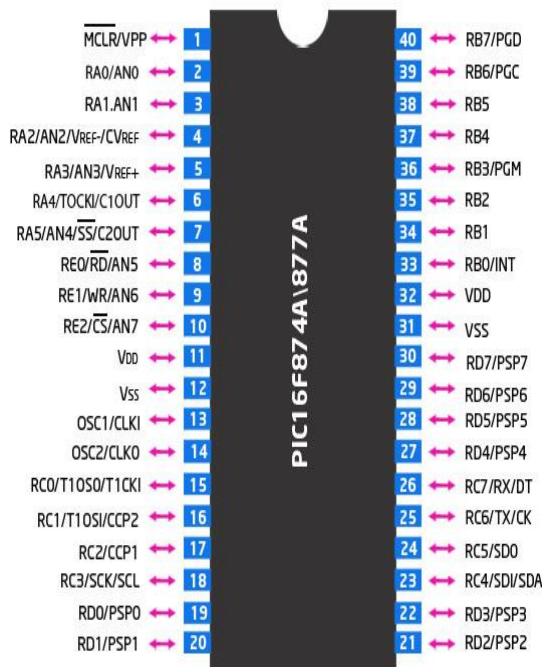
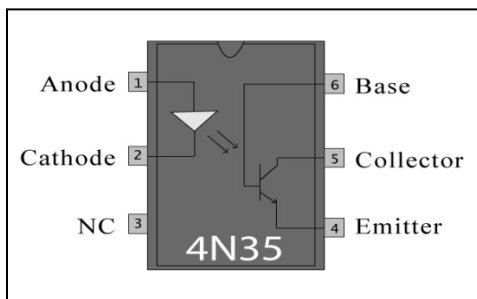


Fig. 5 PIC16F877a

2. OPTO COUPLER

In electronics, an **opto-isolator**, also called an **optocoupler**, **photocoupler**, or **optical isolator**, is "an electronic device designed to transfer electrical signals by utilizing light waves to provide coupling with electrical isolation between its input and output". The main purpose of an opto-isolator is "to prevent high voltages or rapidly changing voltages on one side of the circuit from damaging components or distorting transmissions on the other side." Commercially available opto-isolators withstand input-to-output voltages up to 10 kV and voltage transients with speeds up to 10 kV/μs.

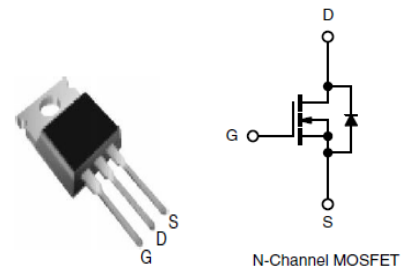
Pin Diagram – 4N35



The LED is a light emitting device and photo transistor is a light sensitive device. The conduction current of phototransistor can be controlled via the conduction current of the LED, even though the two devices are physically separated. Such a package is known as an opto coupler, sine the input (LED) and the output (phototransistor) devices are optically coupled. The most important point to note about the opto coupler device is that a circuit connected to its input can be electrically fully isolated from the output circuit and that a potential difference of hundreds (or) thousands of volts can safely exist between these two circuits without adversely influencing the opto coupler action. This isolating characteristic is the main attraction of this type of opto coupler device, which is generally known as an isolating opto coupler.

3. IRF840

Third generation Power MOSFETs from Vishay provide the designer with the best combination of fast switching, ruggedized device design, low on-resistance and cost-effectiveness. The TO-220AB package is universally preferred for all commercial-industrial applications at power dissipation levels to approximately 50 W. The low thermal resistance and low package cost of the TO-220AB contribute to its wide acceptance throughout the industry.



FEATURES

- Dynamic dV/dt Rating
- Repetitive Avalanche Rated
- Fast Switching
- Ease of Paralleling
- Simple Drive Requirements
- Compliant to RoHS Directive 2002/95/EC

V. RESULTS AND DISCUSSION

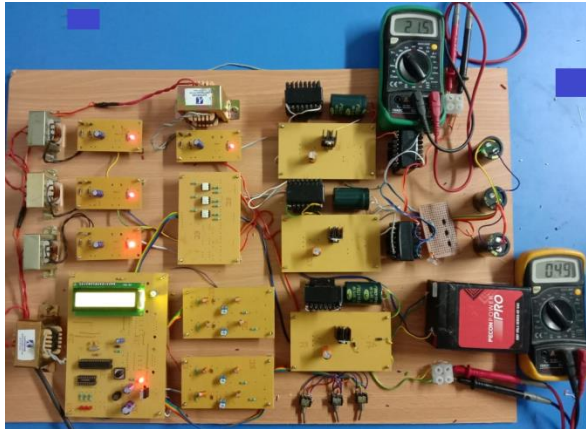


Fig.6 Hardware kit

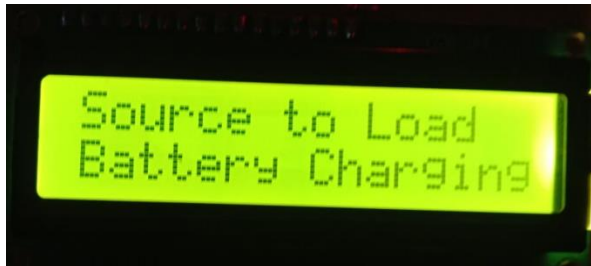


Fig.7 Display for Source to load and battery charging mode



Fig.8 Load voltage



Fig.9 Battery charging voltage

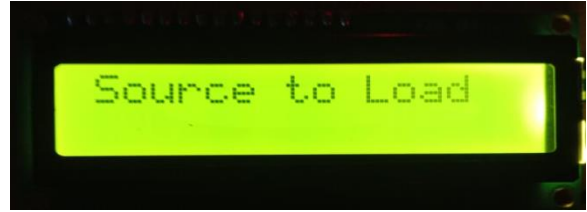


Fig.10 Display for source to Load mode

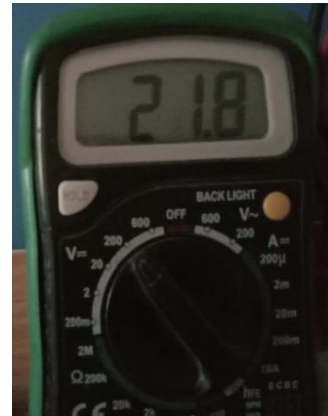


Fig.11 Output voltage for load side in source mode

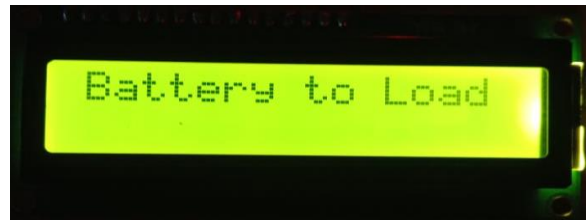


Fig.12 Display for Battery to Load mode



Fig.13 Output voltage for battery mode for load side voltage

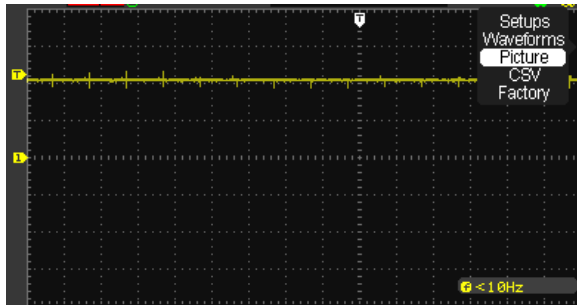


Fig.14 Hardware waveform for source to load side voltage 22.4V

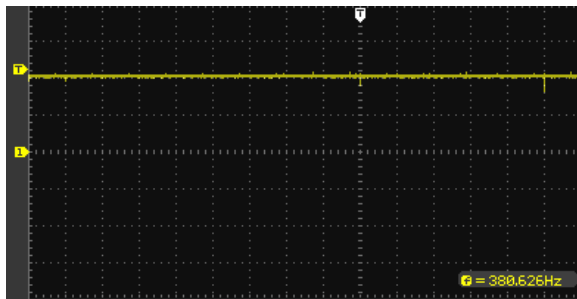


Fig.15 Waveform for battery to load side voltage 22.4V

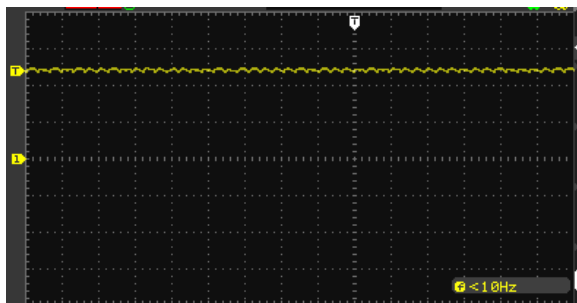


Fig.16 Battery charging voltage waveform 5.8V

VI. CONCLUSION

In order to utilize the three port converters more efficiently in hybrid energy systems, five features have been considered in this paper, which are voltage gain, component sharing, soft switching, number of semiconductors, and current-fed ports. Among the previously introduced converters, few numbers have satisfied two features and only one has met three out of five. Therefore, a partly-isolated three port converter has been introduced in this paper, to meet the features mentioned above effectively. The proposed PITPC has utilized two transformers and two combined voltage-doubler rectifiers, so it has

achieved a high voltage gain. The leakage inductances of the transformers are exploited to make the semiconductors operate with soft switching. The semiconductors soft switching are preserved in all modes, which has led the converter to have good efficiency. Furthermore, the designed PITPC is composed of two boost circuits. As a result, the main input port and the battery port (bidirectional port) are current-fed types, making the proposed PITPC more suitable for renewable energy applications. These two input ports are benefitting from a mutual active clamp circuit. Consequently, the number of semiconductors are decreased. In addition, almost all the components are participating in all of the operating modes, which has led to a cost-efficient converter. Moreover, the PITPC operational mode can be changed by a smooth transition. It has been shown that there is no need for sudden changes in pulse patterns or to use a breaker switch to disconnect a port.

REFERENCES

- [1] S. S. Dobakhshari, J. Milimonfared, M. Taheri, and H. Moradisizkoohi, "A Quasi-Resonant Current-Fed Converter With Minimum Switching Losses," *IEEE Transactions on Power Electronics*, vol. 32, no. 1, pp. 353–362, 2017.
- [2] H. Moradisizkoohi, J. Milimonfared, M. Taheri, and S. Salehi, "A high step-up half-bridge DC/DC converter with a special coupled inductor for input current ripple cancelation and extended voltage doubler circuit for power conditioning of fuel cell systems" *International Journal of Circuit Theory and Applications*, Vol. 44, no. 6, pp. 1290-1307, 2015.
- [3] N. Zhang, D. Sutanto, K. M. Muttaqi "A review of topologies of three-port DC-DC converters for the integration of renewable energy and energy storage system" *Renewable and Sustainable Energy Reviews*, Vol. 56, pp. 388–40, 2016.
- [4] Y.-M. Chen, Y.-C. Liu, and F.-Y. Wu, "Multi-input DC/DC converter based on the multi-winding transformer for renewable energy applications," *IEEE Transactions on Industry Applications*, vol. 38, no. 4, pp. 1096–1104, 2002.
- [5] L. Wang, Z. Wang, and H. Li, "Asymmetrical Duty Cycle Control and Decoupled Power Flow Design of a Three-port Bidirectional DC-DC Converter for Fuel Cell Vehicle Application," *IEEE*

Transactions on Power Electronics, vol. 27, no. 2, pp. 891–904, 2012.

[6] C. Zhao, S. D. Round, and J. W. Kolar, “An Isolated Three-Port Bidirectional DC-DC Converter With Decoupled Power Flow Management,” IEEE Transactions on Power Electronics, vol. 23, no. 5, pp. 2443–2453, 2008.

[7] D. Gunasekaran and L. Umanand, “Integrated magnetics based multi-port bidirectional DC-DC converter topology for discontinuous-mode operation,” IET Power Electronics, vol. 5, no. 7, pp. 935–944, Jan. 2012.

[8] L. Piris-Botalla, G. G. Oggier, and G. O. García, “Extending the power transfer capability of a three-port DC-DC converter for hybrid energy storage systems,” IET Power Electronics, vol. 10, no. 13, pp. 1687–1697, 2017.

[9] B. Chen, Y. Wang, P. Wang, W. Li, F. Han, and L. Yang, “An improved analysis method of loss for the LCLC multi-resonant three-port bidirectional DC-DC converter,” 2018 IEEE Applied Power Electronics Conference and Exposition (APEC), 2018.

[10] J. L. Duarte, M. Hendrix, and M. G. Simoes, “Three-Port Bidirectional Converter for Hybrid Fuel Cell Systems,” IEEE Transactions on Power Electronics, vol. 22, no. 2, pp. 480–487, 2007.

[11] H. Krishnaswami and N. Mohan, “Three-Port Series-Resonant DC-DC Converter to Interface Renewable Energy Sources With Bidirectional Load and Energy Storage Ports,” IEEE Transactions on Power Electronics, vol. 24, no. 10, pp. 2289–2297, 2009.

[12] S. Y. Kim, H.-S. Song, and K. Nam, “Idling Port Isolation Control of Three-Port Bidirectional Converter for EVs,” IEEE Transactions on Power Electronics, vol. 27, no. 5, pp. 2495–2506, 2012.

[13] M. Phatthanasak, R. Gavagsaz-Ghoachani, J. Martin, B. Nahid-Mobarakeh, S. Pierfederici, and B. Davat, “Control of a hybrid energy source comprising a fuel cell and two storage devices using isolated three-port bidirectional DC-DC converters,” 2013 Eighth International Conference and Exhibition on Ecological Vehicles and Renewable Energies (EVER), 2013.

[14] V. N. S. R. Jakka, A. Shukla, and G. D. Demetriades, “Dual-Transformer-Based Asymmetrical Triple-Port Active Bridge (DT-ATAB) Isolated DC-DC Converter,” IEEE Transactions on Industrial Electronics, vol. 64, no. 6, pp. 4549–4560, 2017.

[15] H. Tao, J. Duarte, and M. Hendrix, “Three-Port Triple-Half-Bridge Bidirectional Converter With Zero-Voltage Switching,” IEEE Transactions on Power Electronics, vol. 23, no. 2, pp. 782–792, 2008.